



Article

Large potential of strengthening the land carbon sink in China through anthropogenic interventions

Xu Yue^a, Hao Zhou^b, Yang Cao^c, Hong Liao^{a,*}, Xiaofei Lu^a, Zhen Yu^d, Wenping Yuan^e, Zhu Liu^f, Yadong Lei^g, Stephen Sitch^h, Jürgen Knauerⁱ, Huijun Wang^j

^aJiangsu Key Laboratory of Atmospheric Environment Monitoring and Pollution Control, Jiangsu Collaborative Innovation Center of Atmospheric Environment and Equipment Technology, School of Environmental Science and Engineering, Nanjing University of Information Science & Technology (NUIST), Nanjing 210044, China

^bCollege of Meteorology and Oceanography, National University of Defense Technology, Changsha 410073, China

^cJiangsu Nanjing Environmental Monitoring Center, Nanjing 210013, China

^dKey Laboratory of Agrometeorology of Jiangsu Province, Institute of Ecology, School of Applied Meteorology, NUIST, Nanjing 210044, China

^eInstitute of Carbon Neutrality, Sino-French Institute for Earth System Science, College of Urban and Environmental Sciences, Peking University, Beijing 100871, China

^fDepartment of Earth System Science, Tsinghua University, Beijing 100084, China

^gState Key Laboratory of Severe Weather and Key Laboratory of Atmospheric Chemistry of CMA, Chinese Academy of Meteorological Sciences, Beijing 100081, China

^hCollege of Life and Environmental Sciences, University of Exeter, Exeter EX4 4RJ, UK

ⁱHawkesbury Institute for the Environment, Western Sydney University, Penrith 2751, Australia

^jKey Laboratory of Meteorological Disaster, Ministry of Education, Joint International Research Laboratory of Climate and Environment Change, Collaborative Innovation Center on Forecast and Evaluation of Meteorological Disasters, NUIST, Nanjing 210044, China

ARTICLE INFO

Article history:

Received 23 October 2023

Received in revised form 17 April 2024

Accepted 18 April 2024

Available online 29 May 2024

Keywords:

Carbon sink

Forestation

Ozone

Litter removal

ABSTRACT

The terrestrial ecosystem in China mitigates 21%–45% of the national contemporary fossil fuel CO₂ emissions every year. Maintaining and strengthening the land carbon sink is essential for reaching China's target of carbon neutrality. However, this sink is subject to large uncertainties due to the joint impacts of climate change, air pollution, and human activities. Here, we explore the potential of strengthening land carbon sink in China through anthropogenic interventions, including forestation, ozone reduction, and litter removal, taking advantage of a well-validated dynamic vegetation model and meteorological forcings from 16 climate models. Without anthropogenic interventions, considering Shared Socioeconomic Pathways (SSP) scenarios, the land sink is projected to be 0.26–0.56 Pg C a⁻¹ at 2060, to which climate change contributes 0.06–0.13 Pg C a⁻¹ and CO₂ fertilization contributes 0.08–0.44 Pg C a⁻¹ with the stronger effects for higher emission scenarios. With anthropogenic interventions, under a close-to-neutral emission scenario (SSP1-2.6), the land sink becomes 0.47–0.57 Pg C a⁻¹ at 2060, including the contributions of 0.12 Pg C a⁻¹ by conservative forestation, 0.07 Pg C a⁻¹ by ozone pollution control, and 0.06–0.16 Pg C a⁻¹ by 20% litter removal over planted forest. This sink can mitigate 90%–110% of the residue anthropogenic carbon emissions in 2060, providing a solid foundation for the carbon neutrality in China.

© 2024 Science China Press. Published by Elsevier B.V. and Science China Press. This is an open access article under the CC BY license (<http://creativecommons.org/licenses/by/4.0/>).

1. Introduction

As one of the top CO₂ emitters [1], China is confronted with massive challenges to reaching carbon neutrality. Many mitigation policies and technical solutions have been proposed to cut off emissions and/or to increase sequestrations [2,3]. Among those anthropogenic measures, the potential of ecosystems is less recognized, although they act as the largest carbon sink on land [1]. Currently, the land carbon sink in China is estimated to be 0.2 to 1.1 petagram (Pg) carbon (C) per year [4–6]. The large uncertainty is

in part due to the complexity of the Chinese ecosystem, which covers a wide range of vegetation types, from boreal forests in the north to subtropical forests in the south [7]. The fast growth of atmospheric CO₂ due to anthropogenic emissions provides a strong fertilization effect that drives the ecosystem to a large sink [1]. However, such sink is subject to the changes in both CO₂ and climate, leading to the uncertain potential of land ecosystems for carbon sequestration in the future [8,9].

Many natural climate solutions have been proposed to farm the ecosystem for additional carbon uptake [10]. Among those solutions, forestation (including afforestation and reforestation) has shown the largest potential [10] and has been found to be responsible for large-scale greening [11] and strengthened carbon sinks

* Corresponding author.

E-mail address: hongliao@nuist.edu.cn (H. Liao).

[12,13] in China. However, compared with forestation, other known methods show very limited potential in enhancing ecosystem carbon sinks in China [14]. Considering the water and nutrient constraints on forest expansion [15], it is necessary to explore alternative solutions. Here, we assess the potential of two alternative methods, ozone (O_3) control, and litter removal, in strengthening the land carbon sink in China. Surface O_3 is an air pollutant with its precursors emitted from human activities [16], and it weakens plant photosynthesis due to its strong oxidizing capacity [17,18]. Studies have shown the large benefits of O_3 mitigation on the recovery of ecosystem productivity [19] but have not yet quantified the possible gains in regional carbon sinks. Aboveground litterfall is composed of dead leaves, twigs, bark, and so on. This debris typically decomposes within 1–3 years [20], leading to an increase in soil organic carbon (SOC) and heterotrophic respiration. Although litter removal might have negative impacts on SOC accumulation, field experiments reported that it helped reduce the carbon loss of the whole ecosystem through decreasing soil respiration [21,22].

In this study, we applied the state-of-the-art Yale Interactive terrestrial Biosphere (YIBs) model [23], which was extensively validated with ground-based and satellite observations, to project future changes in the land carbon sink in China at 2060 (averaged for 2050–2064). The model considers the age effect of new plantation with dynamic tree growth through carbon accumulation (Supporting Information 1 online). It also implements a well-established O_3 vegetation damage scheme [18] that has been validated both globally [24] and in China [17]. We performed a total of 1152 simulations, each of which was driven with hourly meteorological forcings derived from one of 16 climate models of the Coupled Model Intercomparison Project phase 6 (CMIP6) under 4 Shared Socioeconomic Pathways (SSPs) in 18 groups of varied configurations. For the land cover change (LCC), we used a recently updated dataset [25] that well captured the trend of forest area in China as reported by national inventories during 1980–2018. We extended the updated LCC to 2100 with assumptions of fast, medium, and slow forestation rates for the future projection of carbon sink. As a comparison, we also used historical LCC at 1850–2014 and future LCC at 2015–2100 under four SSP scenarios from CMIP6 archive [26] to drive the YIBs model. We compared the potentials of strengthening land carbon sinks, measured as net biospheric productivity (NBP), through forestation, O_3 reduction, and litter removal in China

2. Data and methods

2.1. Models

We used the YIBs [23] vegetation model to project future changes in the leaf area index (LAI) and carbon sinks in China. The original YIBs model simulates the leaf photosynthesis [27] and stomatal conductance [28] of eight plant functional types (PFTs), including evergreen broadleaf forest (EBF), evergreen needleleaf forest (ENF), deciduous broadleaf forest (DBF), shrubland, C_3/C_4 grassland, and C_3/C_4 cropland. To account for the separate impacts of LCC in natural (NF) and planted (PF) forests, we added three tree PFTs, including EBF of PF, ENF of PF, and DBF of PF. The leaf-level fluxes are upscaled to the canopy level through integration with the LAI.

The assimilated carbon is allocated to leaves, roots, and wood to support plant development following the mass balance scheme used in the TRIFFID model [29]. In this scheme, the total vegetation carbon density, C_v (kg C m^{-2}), is the sum of leaf biomass C_l , root biomass C_r , and wood biomass C_w , all of which are related to the changes in the balanced LAI, L_b ($\text{m}^2 \text{m}^{-2}$), as follows:

$$C_l = C_r = \sigma \cdot L_b, \quad (1)$$

$$C_w = a_w \cdot L_b^{5/3}, \quad (2)$$

where σ is the PFT-specific leaf carbon density (kg C m^{-2}), and a_w is a PFT-dependent parameter in the power law relating the LAI to wood biomass. The L_b is a function of vegetation height H (m):

$$L_b = b_h \cdot H^{3/2}, \quad (3)$$

where b_h is a PFT-dependent parameter. The actual LAI, L , is related to L_b through a phenological factor p :

$$L = p \cdot L_b. \quad (4)$$

The model updates wood biomass every 10 d as follows:

$$\Delta C_w = \frac{P_{cg}}{1 + \Delta C_l / \Delta C_w + \Delta C_r / \Delta C_w}, \quad (5)$$

where P_{cg} is the accumulated net carbon flux available for growth:

$$P_{cg} = \lambda_g \cdot NPP - \Lambda_l, \quad (6)$$

the parameter λ_g is the fraction of net primary productivity (NPP) available for growth. Λ_l is the total litterfall amount from leaves, roots, and wood calculated as follows:

$$\Lambda_l = \gamma_l \cdot C_l + \gamma_r \cdot C_r + \gamma_w \cdot C_w, \quad (7)$$

where γ_l , γ_r , and γ_w are PFT-dependent conversion parameters related to leaf temperature and soil moisture. As a result, the predicted changes in NPP and Λ_l determine that of wood biomass ΔC_w (Eq. (5)), which is used to update the L_b (Eq. (2)), H (Eq. (3)), L (Eq. (4)), C_l , C_r (Eq. (1)), and the total vegetation carbon C_v . Litterfall Λ_l will be used as input to drive the soil carbon cycle and to predict the changes in soil respiration R_s and soil carbon density. The NBP of the ecosystem is calculated as:

$$NBP = NEP - E_{lcc} = NPP - R_s - E_{lcc}, \quad (8)$$

where E_{lcc} is the emission from LCC. The NEP is net ecosystem productivity, which represents the carbon assimilation by alive vegetation. The age effect of new plantation on NBP is considered (Supporting Information 1 online) and validated against measurements at 27 flux tower sites (Table S1 online). We also designed sensitivity experiments to compare the age effect on land carbon sink from site level to the spatial resolution of $1^\circ \times 1^\circ$ used for this study.

The YIBs model has implemented a flux-based scheme [18] to predict O_3 vegetation damage. In this scheme, the GPP reduction rate F is dependent on the stomatal O_3 flux F_{O_3} above a PFT-dependent threshold T_{O_3} :

$$F = \begin{cases} -a \cdot (F_{O_3} - T_{O_3}), & \text{if } F_{O_3} > T_{O_3}, \\ 0, & \text{if } F_{O_3} \leq T_{O_3}, \end{cases} \quad (9)$$

where a is the damaging sensitivity coefficient, which varies among PFTs with a low or high value to represent the interspecific uncertainties [18]. In this study, we applied the average of the low and high values of a to indicate the mean sensitivity to O_3 damage. The stomatal O_3 flux F_{O_3} is dependent on both stomatal conductance g_s and ambient O_3 concentrations ($[O_3]$):

$$F_{O_3} = \frac{[O_3]}{r_b + k \cdot r_s}, \quad (10)$$

where r_b (s m^{-1}) is the boundary layer resistance and r_s (s m^{-1}) is the stomatal resistance to water ($=1/g_s$). A constant ratio $k=1.67$ is multiplied with r_s to derive the stomatal resistance to O_3 . A higher $[O_3]$ and/or a lower r_s can result in higher stomatal O_3 fluxes and

consequent O₃ damage. We assume no impacts of O₃ on plant respiration, although experiments show that excessive O₃ exposure may enhance vegetation respiration for detoxification [30]. As a result, the O₃ damage effects on the land carbon sink may be underestimated in our simulations.

2.2. Datasets

To validate model performance, we used datasets including satellite-based LAI, a benchmark GPP, 1580 sites of surface O₃, and the national forest inventory. We summarized experimental data from 77 literature about the impacts of litter removal on soil carbon fluxes and nutrients (Supporting Information 2 online). We selected a total of 27 tree sites with age information and at least 10 years of measurements of carbon fluxes and simultaneous meteorology at half-hourly interval from the FLUXNET network (Supporting Information 1 online). We also collected multiple carbon-related variables simulated by 17 (including YIBs) dynamic global vegetation models (DGVMs) from the intercomparison project of trends in the land carbon cycle (TRENDY) [31] (Table S2 online). To drive the YIBs model, we used daily surface meteorology predicted by 16 climate models from the CMIP6 archive (Table S3 online) at both historical (1850–2014) and future (2015–2100) periods under four climate scenarios (Fig. S1 online). All the daily meteorology was downscaled to hourly time step with the diurnal cycle from a reanalysis data product [32]. In addition, we used the ensemble mean surface O₃ concentrations predicted by 13 CMIP6 models (Table S4 online). The monthly mean O₃ was downscaled to hourly time step by applying the seasonal and diurnal cycles from a coupled climate-chemistry-carbon model [23]. All these forcing data were interpolated to the same 1° × 1° resolution as the YIBs model. For details, please refer to Supporting Information 3 (online).

2.3. LCC in China

We used the annual vegetation coverage from both CMIP6 [26] and an inventory-based data product [25] for the present-day simulations. The PFTs of CMIP6 LCC data were converted to YIBs PFTs accordingly (Table S5 online). The original CMIP6 LCC underestimated trends in forest coverage during 1980–2018 compared with the national forest inventory (Fig. 1a). As a result, we adopted a recently updated LCC data product for 1900–2018 that was developed by harmonizing multiple inventory datasets and the high-resolution satellite images in China [25]. This dataset separated the coverage of natural and planted forests, which were further classified into EBF, ENF, and DBF grid by grid using the ratio of PFT cover retrieved by satellites [33] (Fig. S2 online). The new LCC data successfully reproduced the changes of forest cover (Fig. 1a) and other PFTs (Fig. S3 online) as reported by the national inventory. Based on the updated LCC, we generated three future LCC scenarios beyond the year 2018 (Fig. 1a). The LCC1 maintained the same forestation rate as 1980–2018 grid by grid in China, resulting in a continuous forest growth rate of 0.32% a⁻¹ on the national scale. The LCC2 followed LCC1 but with half of the forestation rate at each grid and the national average rate of 0.16% a⁻¹. The LCC3 adopted the same present-day rate but with a maximum cap of 25% for forest area increase in each grid. The LCC3 scenario was designed because recent studies estimated that global reforestation would be limited to 25% due to the constraints of climatic, edaphic, and topographic conditions [15]. With such environmental constraints, the forestation rate in LCC3 is only 0.007% a⁻¹ after the year 2030. For details, please refer to Supporting Information 4 (online).

2.4. Simulations

We performed a total of 1152 runs with the YIBs model. These runs can be aggregated into 18 groups, each of which was forced by different combinations of boundary conditions (Table 1). For all simulations, the YIBs model was run over China with a spatial resolution of 1° × 1° at the hourly time step through the period of 1800–2100. Groups with the prefix of 'ALL' were forced with interannually-varied meteorology and CO₂ concentrations. Groups with the prefix of 'CO₂' ('MET') were the same as 'ALL' runs except that CO₂ concentrations (meteorological variables) after the year 2015 were fixed to the values at 2015. Groups with prefixes of 'O3M' applied the same boundary conditions as 'ALL' runs except that O₃ vegetation damage effects were included with the mean O₃ sensitivities. Groups with prefixes of 'O3F' followed the configurations in 'O3M' except that O₃ concentrations after the year 2015 were fixed to the values at 2015. Groups with prefixes of 'LIT20' or 'LIT50' were the same as 'ALL' runs except that above-ground litter ($\gamma_l \cdot C_l + \gamma_w \cdot C_w$ in Eq. (7), including leaf residue and wood debris) was removed by 20% or 50% before entering the soil carbon pool during 2015–2100. Groups with suffixes of 'LCC1', 'LCC2', 'LCC3', or 'SSP' were forced with land cover datasets from LCC1, LCC2, LCC3, or four CMIP6 SSP scenarios (Fig. 1a). For groups with LCC1, the same land cover data LCC1 were applied for all the four climate scenarios. Similar rules were applied for LCC2 and LCC3 runs. However, for the group with a suffix of 'SSP', four different SSP LCCs (the solid colorful lines in Fig. 1a) were applied under the corresponding climate scenarios. Groups with suffixes of 'FIX15' ('FIX80') were forced with LCC fixed at the year 2015 (1980) thereafter.

We compared the multi-model ensemble mean NBP at 2060 (2050–2064) among different simulations, so as to isolate the contributions by natural (CO₂ or climate) and anthropogenic processes (forestation, O₃ change, or litter removal). The CO₂ effect was quantified as 'ALL_LCC1 – CO2_LCC1' ('ALL_LCC3 – CO2_LCC3') for simulations with LCC1 (LCC3). Similarly, the climatic effect was calculated by 'ALL_LCC1 – MET_LCC1' ('ALL_LCC3 – MET_LCC3'). The contributions of LCC were quantified as 'ALL_LCC1 – ALL_FIX15' and 'ALL_LCC3 – ALL_FIX15' for simulations with LCC1 and LCC3, respectively. The effect of O₃ change was estimated by 'O3M_LCC1 – O3F_LCC1' ('O3M_LCC3 – O3F_LCC3'). The role of litter removal was quantified as 'LIT20_LCC1 – ALL_LCC1' ('LIT20_LCC3 – ALL_LCC3') or 'LIT50_LCC1 – ALL_LCC1' ('LIT50_LCC3 – ALL_LCC3') for different ratios of clearance.

2.5. Validations

The YIBs model joined the TRENDY project and performed favourably against the multimodel ensemble of DGVMs for the global carbon metrics such as GPP, LAI, vegetation biomass, soil carbon, and ecosystem respiration [1]. In this study, we validated the simulated GPP and NEP at global FLUXNET sites (Fig. S4 online) and the GPP and LAI in China (Fig. S5 online). The evaluations showed correlation coefficients of 0.75–0.84 and relative mean biases of 13.5%–18.2% between the ensemble of simulations and observations for GPP and LAI. The simulated NEP showed larger biases with the correlation coefficient of 0.49 and relative mean biases of –55% at 145 sites (Fig. S4b online), because both negative and positive NEPs at observational sites offset each other and lead to a moderate mean NEP of 0.43 g C m⁻² d⁻¹ as the denominator. We further compared the simulated responses of carbon fluxes and the LAI to the changes in CO₂, climate, and land cover with an ensemble of 16 other DGVMs from the TRENDY-v10 project, which provides the same protocols, meteorological forcing, and LCC for all DGVMs. The YIBs model predicted a reasonable mean state of car-

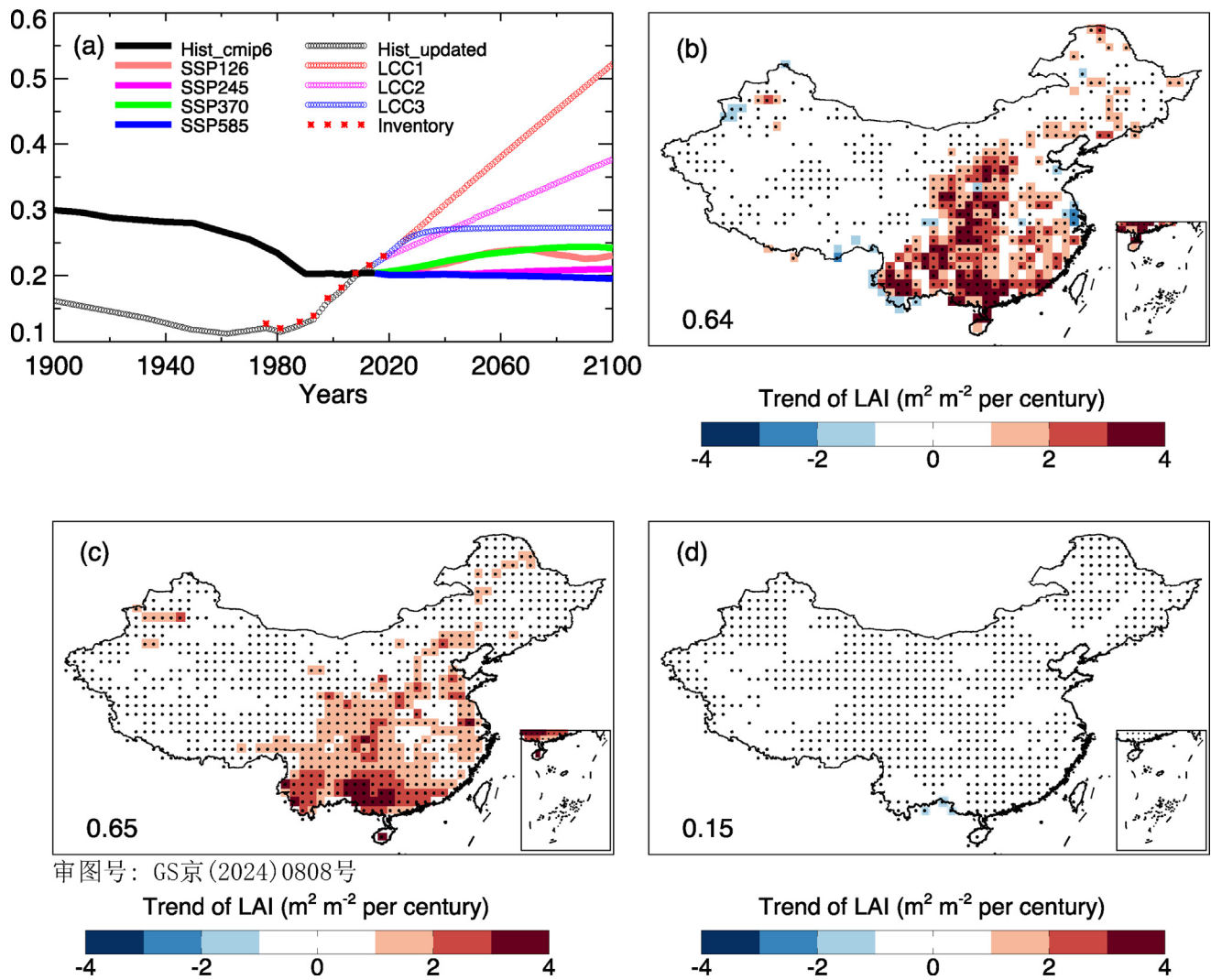


Fig. 1. Comparisons of different land cover changes (LCC) and their impacts on the simulated trends of the leaf area index (LAI). (a) Annual forest coverage in China during 1900–2100 is adopted from the CMIP6 (Hist and SSP scenarios) archive. An updated land cover for 1900–2018 (Hist_updated) is developed [25] based on national inventory (red asterisks). Three updated schemes (LCC1, LCC2, and LCC3) assume varied LCC extending from the Hist_updated data to the year 2100. The trends of the LAI (units: m² m⁻² per century) during 2000–2014 are compared between (b) observations from MODIS satellite retrieval and simulations from the YIBs vegetation model with land cover from the (c) Hist_updated (ALL_LCC1) and (d) CMIP6 Hist datasets (ALL_SSP). The significant trends at the 95% level from (b) observations and (c, d) ensemble mean of simulations are shown with dots. The area-weighted mean trends in the LAI are shown in (b–d).

bon fluxes and LAI during 2000–2014 in China (Table S6 online). Meanwhile, the YIBs model yielded comparable responses of GPP, NBP, and LAI to climate change and LCC relative to other DGVMs (Fig. S6 online). For details, please refer to Supporting Information 5 (online).

3. Results

3.1. Land carbon sink at present

The national inventory showed that forest coverage in China increased from 12.0% during 1977–1981 to 23.0% during 2014–2018, with an average trend of 0.32% a⁻¹ (Fig. 1a). The updated LCC successfully reproduced this observed trend of forest cover change, while the CMIP6 LCC showed only moderate variations in China during 1990–2014. The satellite retrieval revealed a significant greening tendency in China [11], with a mean trend of 0.64 m² m⁻² per century in the LAI during 2000–2014 (Fig. 1b). Driven with the updated LCC, the YIBs model captured the

observed maximum LAI enhancement in the southwest and yielded a national mean trend of 0.65 m² m⁻² per century (Fig. 1c). However, simulations using CMIP6 LCC largely underestimated the increasing trend of LAI (Fig. 1d).

With the updated LCC, the YIBs model predicted a sink of 0.48 Pg C a⁻¹ at present (Fig. 2a). This land sink was equivalent to 27.7% of the national carbon emissions in 2000–2014 and was within the range of 21%–45% estimated by other studies [4–6]. As a comparison, simulations with CMIP6 LCC yielded a weak sink of 0.15 Pg C a⁻¹ in China (Fig. 2b). Such differences of NBP are mainly attributed to that of NEP (Eq. (8)). Inclusion of the observed tendency in forest cover change resulted in a strong NEP of 0.70 Pg C a⁻¹, much higher than that of 0.25 Pg C a⁻¹ for simulations with CMIP6 LCC (Fig. S7 online). The forest in China acts as the major sink, which is in part offset by the carbon loss due to the reduction of shrubland and grassland (Fig. S8 online). The simulation with the updated LCC also captured the historical changes in the national carbon sink, which was lower at 0.17 Pg C a⁻¹ during 1981–2000 and higher at 0.51 Pg C a⁻¹ during 2006–2009, consis-

Table 1
Summary of sensitivity experiments for future projection^a.

| ID | Experiments | CO ₂ | Met | Land cover change ^b | | O ₃ damages ^c | | Litter control ^d | |
|----|-------------|-----------------|-----------|--------------------------------|-----------|-------------------------------------|-----------|-----------------------------|-----------|
| | | | | Types | Variation | Sens | Variation | Reduce | Variation |
| 1 | ALL_LCC1 | 1850–2100 | 1850–2100 | LCC1 | 1850–2100 | None | - | None | - |
| 2 | ALL_LCC2 | 1850–2100 | 1850–2100 | LCC2 | 1850–2100 | None | - | None | - |
| 3 | ALL_LCC3 | 1850–2100 | 1850–2100 | LCC3 | 1850–2100 | None | - | None | - |
| 4 | ALL_FIX80 | 1850–2100 | 1850–2100 | LCC1 | 1850–1980 | None | - | None | - |
| 5 | ALL_FIX15 | 1850–2100 | 1850–2100 | LCC1 | 1850–2015 | None | - | None | - |
| 6 | ALL_SSP | 1850–2100 | 1850–2100 | SSP | 1850–2100 | None | - | None | - |
| 7 | CO2_LCC1 | 1850–2015 | 1850–2100 | LCC1 | 1850–2100 | None | - | None | - |
| 8 | CO2_LCC3 | 1850–2015 | 1850–2100 | LCC3 | 1850–2100 | None | - | None | - |
| 9 | MET_LCC1 | 1850–2100 | 1850–2015 | LCC1 | 1850–2100 | None | - | None | - |
| 10 | MET_LCC3 | 1850–2100 | 1850–2015 | LCC3 | 1850–2100 | None | - | None | - |
| 11 | O3M_LCC1 | 1850–2100 | 1850–2100 | LCC1 | 1850–2100 | Mean | 1850–2100 | None | - |
| 12 | O3M_LCC3 | 1850–2100 | 1850–2100 | LCC3 | 1850–2100 | Mean | 1850–2100 | None | - |
| 13 | O3F_LCC1 | 1850–2100 | 1850–2100 | LCC1 | 1850–2100 | Mean | 1850–2015 | None | - |
| 14 | O3F_LCC3 | 1850–2100 | 1850–2100 | LCC3 | 1850–2100 | Mean | 1850–2015 | None | - |
| 15 | LIT20_LCC1 | 1850–2100 | 1850–2100 | LCC1 | 1850–2100 | None | - | 20% | 2015–2100 |
| 16 | LIT50_LCC1 | 1850–2100 | 1850–2100 | LCC1 | 1850–2100 | None | - | 50% | 2015–2100 |
| 17 | LIT20_LCC3 | 1850–2100 | 1850–2100 | LCC3 | 1850–2100 | None | - | 20% | 2015–2100 |
| 18 | LIT50_LCC3 | 1850–2100 | 1850–2100 | LCC3 | 1850–2100 | None | - | 50% | 2015–2100 |

^a For all simulations, time period is from 1800 to 2100. The forcings at the year before 1850 is fixed to 1850. For runs with forcing during 1850–2100, the input is updated day by day from 1850 to 2100. For runs with forcing during 1850–2015, the input is updated day by day from 1850 to 2015, and then is fixed to the year 2015 thereafter with the annual cycle. For runs with forcing during 1850–1980, the input is updated day by day from 1850 to 1980 and then is fixed to the year 1980 thereafter.

^b For runs driven with LCC1 to LCC3, historical (1900–2018) LCC is adopted from updated LCC [25] and future (2019–2100) is assumed with fast (LCC1), medium (LCC2), and slow (LCC3) forestation rates. For runs driven with CMIP6 LCC, the historical (1850–2014) and future (2015–2100) LCC under four SSP scenarios are applied for corresponding climate scenarios.

^c For O₃ runs, the mean damaging sensitivities are applied.

^d For LIT runs, the reduction of litterfall is applied after the year 2015.

tent respectively with other estimates of 0.19–0.26 Pg C a⁻¹ [5] and 0.39–0.51 Pg C a⁻¹ [34] for the corresponding periods (Fig. 3a).

3.2. Projection of future carbon sink

The SSP inventory projects a high anthropogenic carbon emission of 5.27 Pg C a⁻¹ under the SSP5–8.5 scenario and a low emission of 0.52 Pg C a⁻¹ under the SSP1–2.6 scenario in China at 2060. We explored how much of these emissions could be mitigated by ecosystems. With fixed forest cover at the year 2015, the land carbon sink in 2060 is projected to be 0.26 Pg C a⁻¹ under SSP1–2.6 and 0.56 Pg C a⁻¹ under the SSP5–8.5 scenario ('ALL_FIX15' in Table S7 online), equivalent to 50.0% and 10.6% of the corresponding carbon emissions, respectively. At 2060, the land carbon sink is 0.53 Pg C a⁻¹ with LCC1 and SSP1–2.6 climate (Fig. 2c and 'ALL_LCC1' in Table S7 online), almost equal to the total anthropogenic emissions in China under the same scenario. Such a sink will be 0.87 Pg C a⁻¹ under the SSP5–8.5 scenario but account for only 16.4% of the contemporary carbon emissions (Fig. 2d). As a comparison, with a conservative forestation rate (LCC3), the national carbon sink will be 0.38 Pg C a⁻¹ under SSP1–2.6 (Fig. 2e) and 0.70 Pg C a⁻¹ under the SSP5–8.5 (Fig. 2f) scenario ('ALL_LCC3' in Table S7 online).

With the same LCC (either LCC1 or LCC3), the national sink in 2060 is 0.33 ± 0.01 Pg C a⁻¹ higher under SSP5–8.5 than under SSP1–2.6 scenario (Fig. 2g). The fast CO₂ growth rates under the SSP3–7.0 and SSP5–8.5 scenarios (Fig. S1 online) help promote the sink by 0.32–0.44 Pg C a⁻¹ compared with the present day (Fig. 2h and Table 2) through CO₂ fertilization. In contrast, the slow CO₂ growth rates under the SSP1–2.6 and SSP2–4.5 scenarios moderately strengthen the sink by 0.08–0.21 Pg C a⁻¹ (Table 2). Changes in climatic factors, including temperature, radiation, and soil moisture (Fig. S1 online), jointly strengthen the land carbon sink by 0.06–0.13 Pg C a⁻¹ with some inter-model spreads (Fig. 2i and Table 2). As a result, CO₂ fertilization rather than climate change dominates the future carbon sink if there are no anthropogenic interventions.

3.3. Impacts of forestation, O₃ reduction, and litter removal

Compared with the simulations with fixed land cover after the year 1980 ('ALL_FIX80'), when the actual forest coverage began to increase (Fig. 1a), the YIBs model driven with the updated LCC showed a larger NBP of 0.26 Pg C a⁻¹ at 2010 (Fig. 3d). This gain in carbon sink did not appear before the year 2000 because the conversion of shrubland and grassland to forest resulted in carbon emissions (Fig. S8d and e online) while the low NBP of newly-planted trees could not compensate for such carbon loss. The disturbance-induced carbon source turned into a sink within 20 years, a period consistent with observations [35]. At 2060, the NBP with continuous forestation in LCC1 ('ALL_LCC1') becomes 0.53–0.87 Pg C a⁻¹ for different climate scenarios (Fig. 3a). As a moderate case, the application of LCC2 ('ALL_LCC2') results in a sink of 0.46–0.79 Pg C a⁻¹ (Fig. 3b). The slow increases in forest coverage in LCC3 ('ALL_LCC3') result in a sink of 0.38–0.70 Pg C a⁻¹ at 2060 (Fig. 3c). Compared with the simulations with fixed 2015 land cover ('ALL_FIX15'), these runs showed enhancements in NBP of 0.29 ± 0.02 Pg C a⁻¹ for LCC1 (Fig. 3g), 0.22 ± 0.02 Pg C a⁻¹ for LCC2 (Fig. 3h), and 0.13 ± 0.01 Pg C a⁻¹ for LCC3 (Fig. 3i). Different from the negative effects in NBP by LCC in the 1980s (Fig. 3d–f), the forestation after 2015 always promotes NBP (Fig. 3g–i) because of the strong carbon uptake by middle-age trees planted in 1980–2015. Such gains in carbon sink retain for decades even for the LCC3 with the cease of forestation after 2030 (Fig. 1a), and show limited variations among climate scenarios (Fig. 3g–i).

We then examined the effects of O₃ mitigation on the land carbon sink based on the ensemble mean O₃ concentrations from 13 CMIP6 models. The O₃ pollution is estimated to reduce the national gross primary productivity (GPP) by 6.7% and the LAI by 1.8% at present [9]. Such damaging effect resulted in a loss of 0.1 Pg C a⁻¹ (20.8%) for the present-day NBP ('O3M_LCC1' minus 'ALL_LCC1' in Table S7 online), mainly attributed to the damage of 0.05 Pg C a⁻¹ for natural forest (NF) and 0.04 Pg C a⁻¹ for planted forest (PF). Relative to 2010, the O₃ concentration in 2060 averaged

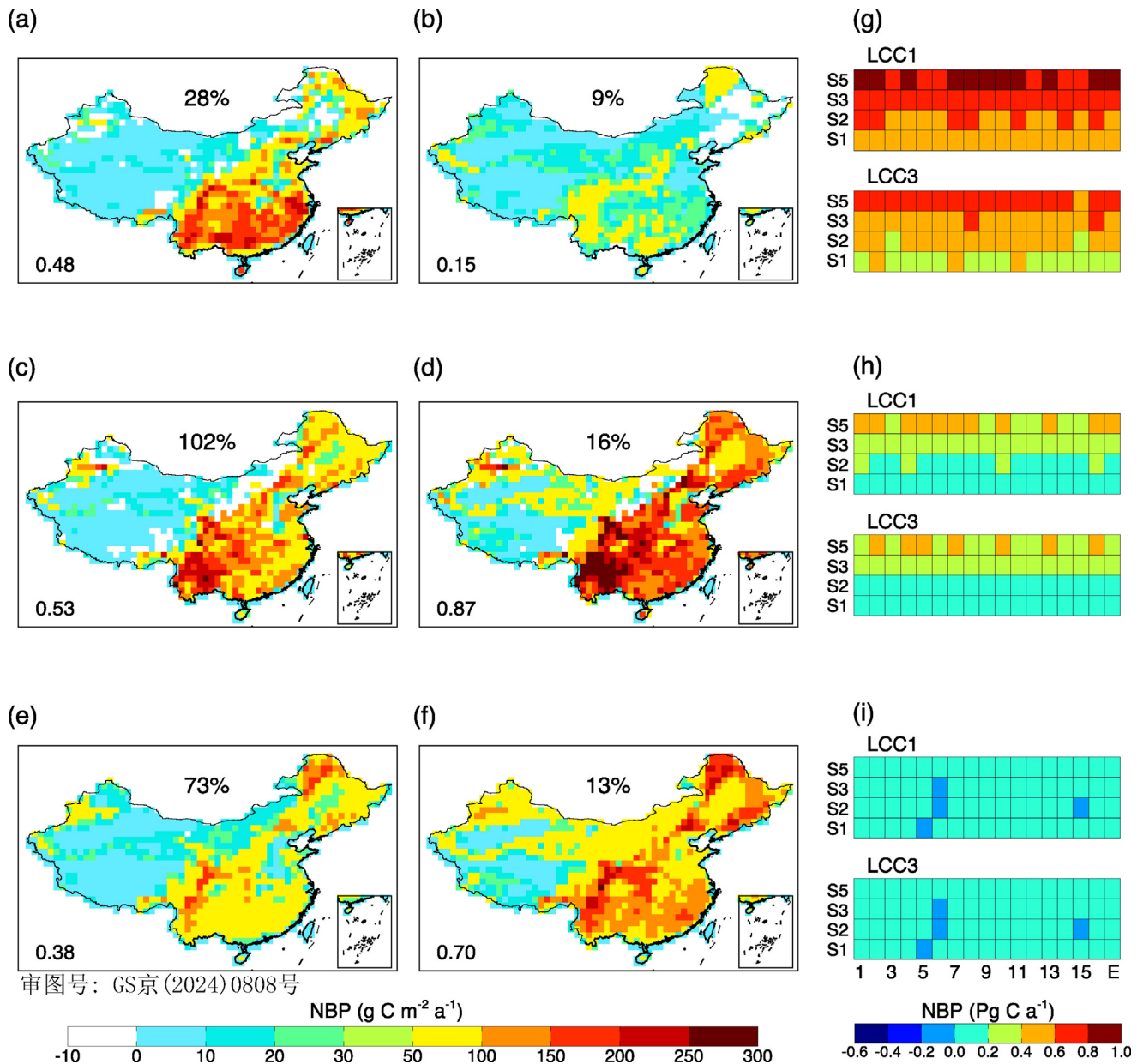


Fig. 2. Prediction of land carbon sink in China and its contributions by CO₂ fertilization and climate change. The ensemble mean net biospheric productivity (NBP) in 2010 is simulated with historical LCC from the (a) updated (ALL_LCC1) and (b) CMIP6 (ALL_SSP) datasets. The carbon sinks in 2060 are projected using the LCC datasets from (c, d) LCC1 (ALL_LCC1) and (e, f) LCC3 (ALL_LCC3) schemes and climate forcing from (c, e) SSP1-2.6 and (d, f) SSP5-8.5 scenarios. The effects of O₃ vegetation damage and litter removal are not included. Positive (negative) values indicate a carbon sink (source) with significant changes at the 95% level over almost all grids. The area-weighted total carbon sink (Pg C a⁻¹) and its ratio to contemporary carbon emissions (%) are shown on each panel of (a–f). The simulated total carbon sink at 2060 with climate from 16 CMIP6 models and four different climate scenarios are shown in the right panel with (g) all forcing, (h) CO₂ fertilization alone, and (i) climate change alone under either LCC1 or LCC3 schemes. Each number in (g–i) indicates one climate model, and ‘E’ represents their ensemble mean.

over the growth season and over China is projected to decrease 10.2 ppbv (–17.6%) under the SSP1-2.6 scenario and 1.3 ppbv (–2.2%) under the SSP2-4.5 scenario, with maximum reductions in the southeast (Fig. S9 online). Following such a tendency, the land carbon sink shows increases of 0.08 Pg C a⁻¹ under SSP1-2.6 and 0.04 Pg C a⁻¹ under SSP2-4.5 (Table 2). In contrast, the average O₃ increases 8.6 ppbv (14.9%) under SSP3-7.0 and 7.5 ppbv (13.0%) under SSP5-8.5 (Fig. S9 online), leading to NBP reductions of 0.02 Pg C a⁻¹ in both scenarios (Table 2). The responses of GPP to O₃ are nonlinear, with slower GPP reduction rates at higher O₃ levels [24]. Furthermore, the smallest stomatal conductance is predicted under SSP5-8.5 (Fig. S10 online) following the warmest climate (Fig. S11 online), the lowest relative humidity (Fig. S12 online), and the highest CO₂ concentrations (Fig. S1a online). Both

dry air and high CO₂ inhibit stomatal conductance [36,37], leading to smaller responses of the land carbon sink to O₃ under SSP5-8.5. On average, for the same O₃ reduction of 10 ppbv, the highest efficiency of 0.09 Pg C a⁻¹ is predicted under the SSP1-2.6 scenario (Fig. 4a), while the lowest efficiency of 0.03 Pg C a⁻¹ is predicted under the SSP5-8.5 scenario (Fig. 4b).

We found large benefits of litter removal in strengthening land carbon sinks. With a 20% reduction in aboveground litterfall for all vegetation types over each grid, an increase of 0.68 to 0.77 Pg C a⁻¹ in NBP is achieved under varied climate scenarios and LCCs in 2060 relative to simulations without litter removal (Table 2). Such change is contributed by a 13% reduction in soil respiration, which is not sensitive to climate scenarios (Figs. S13, S14 online). The sensitivity experiment with a 50% reduction in litter causes an even

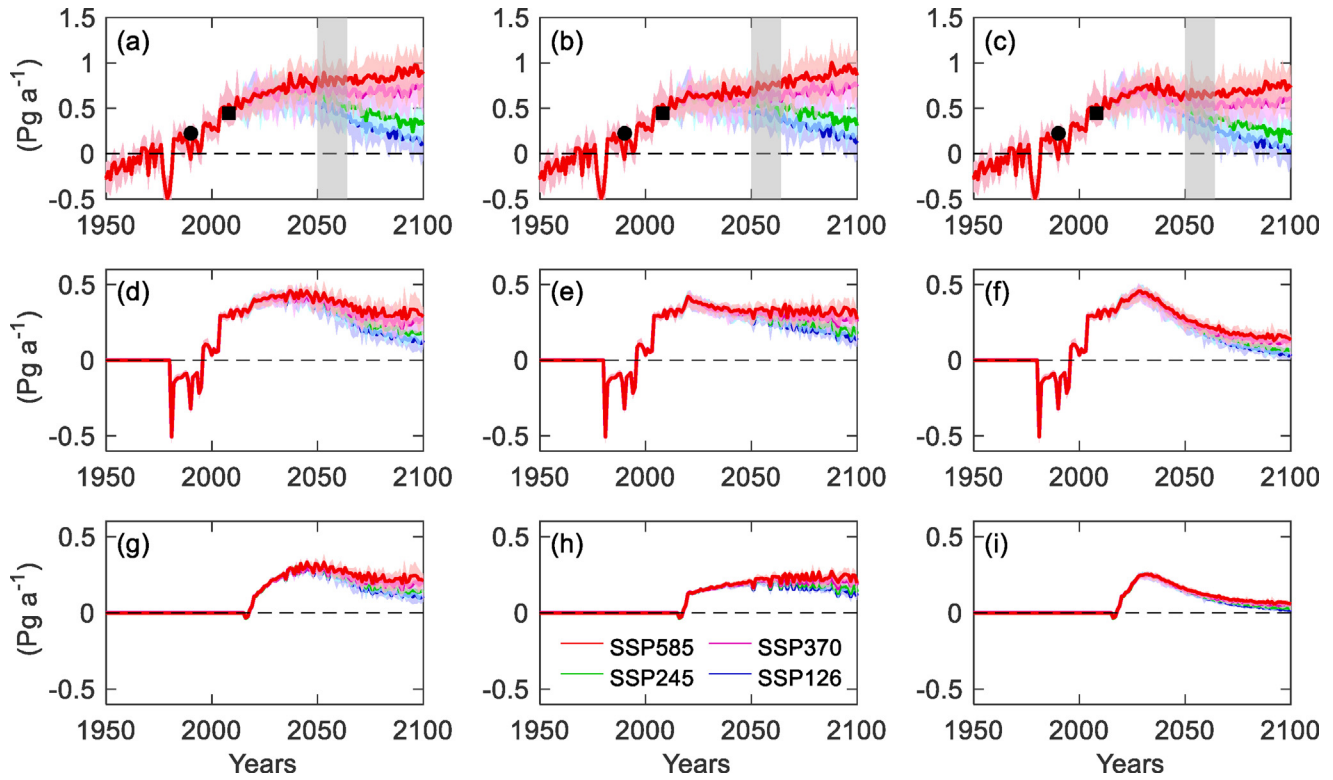


Fig. 3. Prediction of land carbon sink and its contributions by LCC in China for 1950–2100. Results shown are the ensemble mean NBP predicted by the YIBs model driven with climate from 16 CMIP6 models under four SSP scenarios under (a) LCC1, (b) LCC2, (c) LCC3 schemes. The effects of O₃ vegetation damage and litter removal are not included. The two black symbols represent the carbon sink for 1980–2000 [5] and 2006–2009 [34] in China estimated with observation-based approaches. The differences of NBP between the simulations with year-to-year varied LCC and those with fixed LCC after the year (d–f) 1980 (ALL_FIX80) and (g–i) 2015 (ALL_FIX15) indicate the contributions of LCC to regional carbon sink after the specific years. The (d, g) LCC1, (e, h) LCC2, and (f, i) LCC3 schemes are applied in the year-to-year varied LCC simulations, respectively. The colorful shadings indicate the uncertainties due to the climatic forcing from different CMIP6 models. The grey shadings in (a–c) indicate the period of 2050–2064 for the future projection.

Table 2
Summary of NBP (Pg C a⁻¹) at 2060 and its changes by different forcings^a.

| ID | NBP and its changes | SSP1-2.6 | SSP2-4.5 | SSP3-7.0 | SSP5-8.5 |
|-----|------------------------------------|---------------------------|---------------------------|-----------------------------|-----------------------------|
| (1) | NBP with all forcings ^b | 0.54 ± 0.05 (0.41 ± 0.04) | 0.61 ± 0.05 (0.48 ± 0.04) | 0.68 ± 0.03 (0.55 ± 0.03) | 0.79 ± 0.05 (0.65 ± 0.04) |
| (2) | The sum of ΔNBP in (3)–(6) | 0.51 ± 0.08 (0.33 ± 0.06) | 0.61 ± 0.07 (0.43 ± 0.05) | 0.69 ± 0.05 (0.50 ± 0.04) | 0.86 ± 0.06 (0.65 ± 0.05) |
| (3) | ΔNBP by CO ₂ | 0.09 ± 0.01 (0.08 ± 0.01) | 0.21 ± 0.01 (0.20 ± 0.01) | 0.34 ± 0.02 (0.32 ± 0.02) | 0.44 ± 0.03 (0.42 ± 0.03) |
| (4) | ΔNBP by climate | 0.07 ± 0.05 (0.06 ± 0.05) | 0.08 ± 0.05 (0.07 ± 0.04) | 0.08 ± 0.04 (0.07 ± 0.03) | 0.13 ± 0.03 (0.11 ± 0.03) |
| (5) | ΔNBP by LCC | 0.27 ± 0.02 (0.12 ± 0.01) | 0.28 ± 0.02 (0.13 ± 0.01) | 0.29 ± 0.02 (0.13 ± 0.01) | 0.31 ± 0.02 (0.14 ± 0.01) |
| (6) | ΔNBP by O ₃ | 0.08 ± 0.01 (0.07 ± 0.01) | 0.04 ± 0.00 (0.03 ± 0.00) | -0.02 ± 0.00 (-0.02 ± 0.00) | -0.02 ± 0.00 (-0.02 ± 0.00) |
| (7) | ΔNBP by -20% litter of PF | 0.20 ± 0.01 (0.16 ± 0.01) | 0.20 ± 0.01 (0.17 ± 0.01) | 0.21 ± 0.01 (0.17 ± 0.01) | 0.21 ± 0.01 (0.17 ± 0.01) |

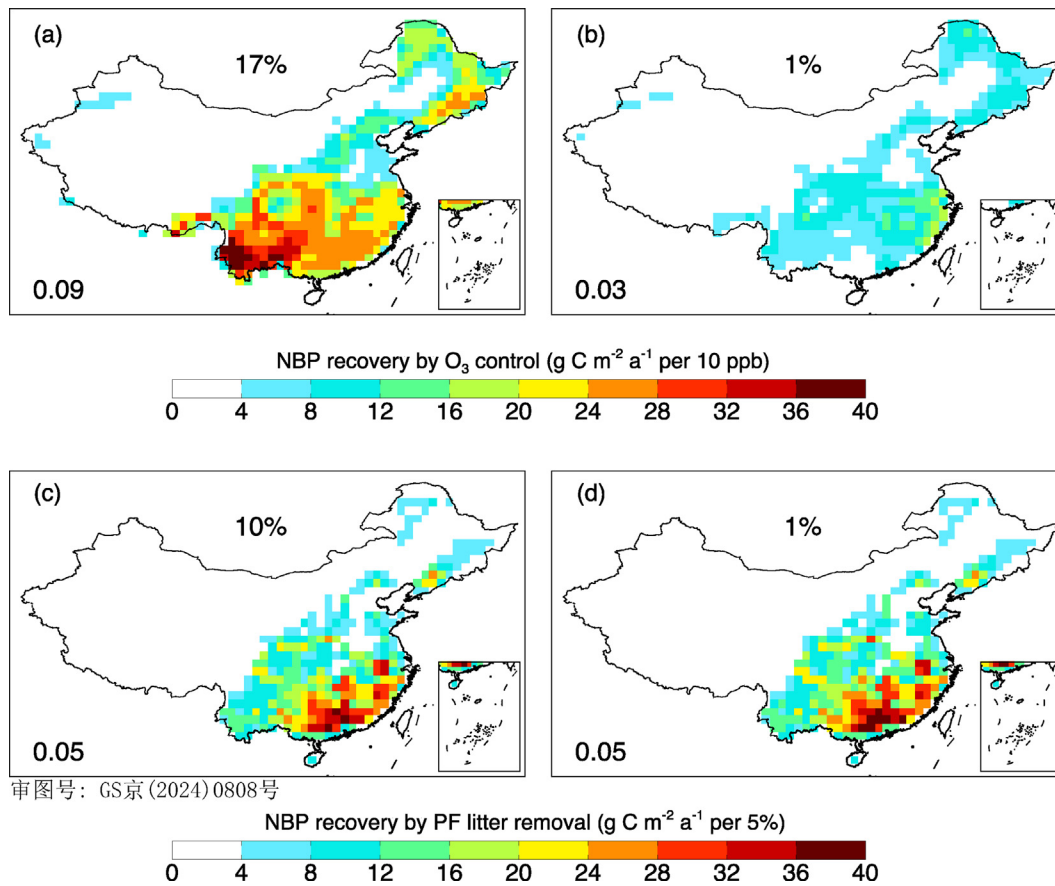
^a The NBP changes (ΔNBP) ± uncertainties are derived as the differences between varied sensitivity experiments (Table S7 online). The uncertainties are indicated as one standard deviation of results driven with 16 CMIP6 models. Both the ΔNBP with LCC1 and LCC3 (in bracket) are shown.

^b The same as the NBP from the O3M_LCC1 and O3M_LCC3 experiments.

larger decline of 33% in soil respiration, leading to the stronger NBP enhancements of 1.70 to 1.93 Pg C a⁻¹ (Table S7 online). A meta-analysis of 77 experiments worldwide showed that 100% litter removal on average decreased soil respiration by 23% (Fig. S15 online). Our simulated responses of soil respiration (reduction of 66% with 100% litter removal) to litter removal are about 3 times observations, likely because the YIBs model overestimates the amount of aboveground litterfall while omits the additional decomposition of SOC by soil microbes (Supporting Information 2 online). Given the unclear long-term perturbations to the projected ecosystems, we suggest that the application of litter removal should be limited to PF. Averaged for both climate models and scenarios, the removal of 5% of litter of the PF can increase the national carbon sink by 0.05 Pg C a⁻¹ in our simulation, with the maximum benefits in southeastern China, where most of PF is located (Fig. 4c and d).

4. Discussion

The projection of future carbon sinks showed uncertainties due to the differences in CO₂ concentrations, climate change, and anthropogenic interventions. We found the largest uncertainty from the CO₂ scenarios with an NBP fluctuation ranging from 0.08 to 0.44 Pg C a⁻¹ (Table 2), followed by the uncertainty of 0.12–0.31 Pg C a⁻¹ due to varied LCC assumptions. The NBP range induced by climate change was relatively small at 0.06–0.13 Pg C a⁻¹, even lower than that of -0.02 to 0.08 Pg C a⁻¹ caused by O₃ damages and 0.68 to 0.77 Pg C a⁻¹ by litter removal under varied scenarios. As a comparison, the meteorological forcings from different climate models cause limited uncertainties in NBP compared with the mean NBP changes (Table 2). The projection is also affected by the biases in the vegetation model. Site-level evaluations showed that YIBs model predicted lower NEP than



审图号: GS京(2024)0808号

Fig. 4. Changes of land carbon sink in China in 2060 by O₃ pollution control and litter removal of planted forest (PF). Results shown are the ensemble mean changes of the land carbon sink in 2060 caused by (a, b) each 10 ppb decrease in surface O₃ and (c, d) each 5% reduction in litterfall of PF under the (a, c) SSP1-2.6 and (b, d) SSP5-8.5 climate scenarios. Positive (negative) values indicate an increase (decrease) in the carbon sink. The area-weighted total carbon sink (Pg C a⁻¹) and its ratio to contemporary carbon emissions (%) are shown in each panel.

observations (Fig. S4b online), suggesting that the strength of carbon sink may be underestimated for future projection.

Our findings broadly align with previous studies on the impacts of afforestation, climate change, and CO₂ fertilization on carbon sequestration. For instance, Yao et al. [8] projected that forest biomass carbon sequestration would assimilate 0.17 Pg C a⁻¹ from 2000 to 2040, taking into account CO₂ fertilization, climate change, and the aging of forests without expanding forested areas. As a comparison, our simulations with fixed LCC after 2015 yielded a lower sink of 0.13 Pg C a⁻¹ in 2000–2040 by the biomass carbon accumulation. Qiu et al. [38] estimated that national forest coverage would increase from 22.8% in 2003 to 30.9% in 2050, equivalent to an average LCC rate of 0.17% a⁻¹ which is similar to our LCC2 assumption. They predicted that the increase of forest biomass would provide an average carbon sink of 0.19 Pg C a⁻¹ during 2020–2050 in China. In our prediction, the land carbon sink with LCC2 is 0.61 ± 0.05 Pg C a⁻¹ during 2020–2050 (Fig. 3b), with vegetation biomass alone contributing 0.21 ± 0.01 Pg C a⁻¹, closely matching the estimate of Qiu et al. [38]. Recently, Huang et al. [39] assumed a medium LCC rate of 0.16% a⁻¹ for 2020–2050 and projected that the ecosystem in China would sequester 0.46 ± 0.10 Pg C a⁻¹ under RCP2.6 and 0.49 ± 0.11 Pg C a⁻¹ under RCP4.5 scenario in the 2050s. These numbers are comparable to our estimates of 0.46 ± 0.05 Pg C a⁻¹ under SSP1-2.6 and 0.56 ± 0.05 Pg C a⁻¹ under SSP2-4.5 scenarios with LCC2 by 2060 (Table S7 online).

We found large potential of increasing carbon sequestration by forestation, which enhances national 2060 NBP by 0.27–0.31

Pg C a⁻¹, 0.20–0.23 Pg C a⁻¹, 0.12–0.14 Pg C a⁻¹ with the fast (0.32% a⁻¹), medium (0.16% a⁻¹), and slow (0.007% a⁻¹ after 2030) LCC, respectively (Table 2). The recent study of Xu et al. [40] also predicted a sizable sink of 0.27 Pg C a⁻¹ by new plantation at a rate of 0.2% a⁻¹ for 2020–2060, very close to our estimate with the LCC2 assumption. In contrast, Cai et al. [41] projected that the existing forest accounted for more than 90% of the ecosystem carbon sink with limited contributions by new forestation. Such discrepancy may be caused by the differences of projection tools as both Xu et al. [40] and this study used the DGVMs while Cai et al. [41] applied the empirical models based on logistic growth equations. In addition to this uncertainty, the implementation of forestation is subject to labor costs and is confronted with possible side effects. Forestation is limited by plantation areas and environmental constraints such as water and nutrient availability [15]. The new plantations may introduce unexpected environmental stresses [42], limiting the possibility of stable forestation rates. As a result, the moderate or conservative forestation schemes such as LCC2 and LCC3 are more likely to be implemented in the future. The full benefit of forestation can be achieved by 70% and 90% at the expense of 50 and 100 USD per ton CO₂ [43], respectively, suggesting the high cost of this approach.

Compared with forestation, O₃ reduction seems to have low efficiency, as the significant reduction of 10 ppbv in surface O₃ can mitigate only 0.03–0.09 Pg C a⁻¹ in China (Fig. 4a, b). In addition, the amelioration of O₃ control is sensitive to climatic scenarios with moderate effects under warmer and drier climates. Despite these drawbacks, the NBP recovery from O₃ reduction is

the most feasible target, as the national 90th percentile O₃ level is projected to decrease >20 ppbv at the year 2060 [44] following low-carbon-policy scenarios [45]. The benefits of an enhanced carbon sink will be sustained as long as the O₃ level remains low. Furthermore, we assumed no impacts of O₃ on plant respiration, though field experiments showed that excessive O₃ exposure may enhance vegetation respiration for detoxification [30]. As a result, the recovery of carbon sink by O₃ reduction may be underestimated in our simulations. Studies estimated that 90% reduction of NO_x in China, the most effective way to mitigate surface O₃ [46], would cost 65 billion USD [47]. Assuming the O₃ regulation takes effect through 2015–2060, we calculated an accumulative recovery of 2.06 Pg C ('O3M_LCC3' minus 'O3F_LCC3') in carbon sink by O₃ control and a net cost of 8.6 USD per ton CO₂ during the 46-year period. This is a relatively low-cost solution with large benefits for both ecosystem and public health.

Litter removal is an efficient way to increase the carbon sequestration of existing forests, especially when the forestation is limited by the available land. However, litter removal reduces the input of nutrients such as nitrogen and phosphorus to the soil. Our meta-analysis showed that 100% litter removal decreased total soil nitrogen by 13% and total phosphorus by 12% (Supporting Information 2 online). The long-term impacts of these perturbations on ecosystem functions deserve further investigations. In practice, we suggest conservative ratios of litter removal with appropriate fertilization [48,49] to maintain the biodiversity, microbial community, and biogeochemical properties of ecosystems. Meanwhile, the "Natural Forest Protection Project" in China may not allow any anthropogenic perturbations to the natural forests, limiting the action of litter removal to PF alone. Here, we calculated the perturbed NBP with 20% litter removal over PF alone and yielded an increase of 0.16–0.21 Pg C a⁻¹ in land carbon sink at 2060 (Table 2). This sink is adjusted to 0.06–0.07 Pg C a⁻¹ if scaled by the observed changes in soil respiration from meta-analysis (Fig. S15a online) to that from simulations (Figs. S13, S14 online). The collected litterfall can be used as bioenergy to substitute fossil fuels [50] to reduce anthropogenic CO₂ emissions [51], or buried deep into soil to preserve vegetation carbon for decades without perturbations of soil nutrients [52]. The cost of litter removal consists of collection, transportation, and transformation/bury. Recent studies estimated a cost of 30 USD per ton CO₂ for wood vault [52] and 14 USD per ton CO₂ for crop residual bury [53], both of which are much lower than the cost of carbon capture, utilization and storage (CCUS) through geological storage [54].

With over 70 countries' net-zero pledges by 2050–2070, recent projections showed that the temperature rise in the 2100s can be limited to below 2 °C above the preindustrial level [55], very similar to the warming pathway assumed by the SSP1-2.6 scenario [56]. However, even for such a green scenario, the net carbon emission is not zero. To achieve carbon neutrality, negative emissions are required in addition to the improved efficiencies and renewables development [3]. Our study shows that anthropogenic interventions to the ecosystems can act as an important measure of negative emissions by strengthening land carbon sinks in China. Forestation can help increase 0.12 Pg C a⁻¹ in the national carbon sink at 2060 even with a low LCC rate due to environmental constraints (LCC3, Table 2). Together with the O₃ pollution control (0.07 Pg C a⁻¹) and the annual removal of 20% litter over PF (0.16 Pg C a⁻¹, or 0.06 Pg C a⁻¹ if adjusted), we expect an additional carbon uptake of 0.25–0.35 Pg C a⁻¹ through anthropogenic interventions at 2060. This benefit, nonlinearly coupled with the baseline sink due to CO₂ fertilization and climate change, result in a sizable sink of 0.47–0.57 Pg C a⁻¹ (The NBP in 'O3M_LCC3' plus litter removal) by the ecosystem under the SSP1-2.6 scenario. This sink can mitigate 90%–110% of the residue anthropogenic CO₂ emissions at 2060 in China under the same scenario. In addition,

other natural climate solutions such as forest management, crop-land nutrient management, and grazing optimization can further enhance the potential of terrestrial carbon sink [43]. Therefore, our study suggests an achievable target for reaching national carbon neutrality with contributions by the ecosystems.

Conflict of interest

The authors declare that they have no conflict of interest.

Acknowledgments

This work was supported by the National Natural Science Foundation of China (42293323 and 42275128) and the Natural Science Foundation of Jiangsu Province (BK20220031). We thank all the DGVM authors in TRENDY-v10 project for providing the long-term simulation data.

Author contributions

Xu Yue, Hong Liao, and Huijun Wang conceived the study. Xu Yue designed the research and performed simulations. Hao Zhou generated the updated and future LCC for simulations. Yang Cao collected the age information of FLUXNET sites. Xiaofei Lu performed the meta-analysis for the ecological impacts of litter removal. Zhen Yu provided the inventory-based LCC data in China. Xu Yue and Hong Liao led the writing and revision of the paper, with contributions from Wenping Yuan, Zhu Liu, Yadong Lei, Stephen Sitch, and Jürgen Knauer.

Appendix A. Supplementary materials

Supplementary materials to this article can be found online at <https://doi.org/10.1016/j.scib.2024.05.037>.

Data availability

The links and references of all observational data have been shown in Supporting Information 3. The CMIP6 data is available at <https://esgf-node.llnl.gov/>. The simulated NBP in China from all experiments with the YIBs model is available at <https://doi.org/10.6084/m9.figshare.21931119>.

References

- [1] Friedlingstein P, O'Sullivan M, Jones MW, et al. Global carbon budget 2020. *Earth Syst Sci Data* 2020;12:3269–340.
- [2] Wang F, Harindintwali JD, Yuan Z, et al. Technologies and perspectives for achieving carbon neutrality. *Innovation* 2021;2:100180.
- [3] Liu Z, Deng Z, He G, et al. Challenges and opportunities for carbon neutrality in China. *Nat Rev Earth Environ* 2022;3:141–55.
- [4] Fang JY, Guo ZD, Piao SL, et al. Terrestrial vegetation carbon sinks in China, 1981–2000. *Sci China Ser D Earth Sci* 2007;50:1341–50.
- [5] Piao S, Fang J, Ciais P, et al. The carbon balance of terrestrial ecosystems in China. *Nature* 2009;458:1009–13.
- [6] Wang J, Feng L, Palmer PI, et al. Large Chinese land carbon sink estimated from atmospheric carbon dioxide data. *Nature* 2020;586:720–3.
- [7] Fang JY, Yu GR, Liu LL, et al. Climate change, human impacts, and carbon sequestration in China. *Proc Natl Acad Sci USA* 2018;115:4015–20.
- [8] Yao YT, Piao SL, Wang T. Future biomass carbon sequestration capacity of Chinese forests. *Sci Bull* 2018;63:1108–17.
- [9] Yue X, Liao H, Wang H, et al. Pathway dependence of ecosystem responses in China to 1.5°C global warming. *Atmos Chem Phys* 2020;20:2353–66.
- [10] Griscom BW, Adams J, Ellis PW, et al. Natural climate solutions. *Proc Natl Acad Sci USA* 2017;114:11645–50.
- [11] Chen C, Park T, Wang XH, et al. China and India lead in greening of the world through land-use management. *Nat Sustain* 2019;2:122–9.
- [12] Yue X, Zhang T, Shao C. Afforestation increases ecosystem productivity and carbon storage in China during the 2000s. *Agric For Meteorol* 2021;296:108227.

- [13] Lu F, Hu HF, Sun WJ, et al. Effects of national ecological restoration projects on carbon sequestration in China from 2001 to 2010. *Proc Natl Acad Sci USA* 2018;115:4039–44.
- [14] Qin ZC, Deng X, Griscom B, et al. Natural climate solutions for China: The last mile to carbon neutrality. *Adv Atmos Sci* 2021;38:889–95.
- [15] Bastin JF, Finegold Y, Garcia C, et al. The global tree restoration potential. *Science* 2019;365:76–9.
- [16] Li K, Jacob DJ, Liao H, et al. Anthropogenic drivers of 2013–2017 trends in summer surface ozone in China. *Proc Natl Acad Sci USA* 2019;116:422–7.
- [17] Yue X, Unger N, Harper K, et al. Ozone and haze pollution weakens net primary productivity in China. *Atmos Chem Phys* 2017;17:6073–89.
- [18] Sitch S, Cox PM, Collins WJ, et al. Indirect radiative forcing of climate change through ozone effects on the land-carbon sink. *Nature* 2007;448:791–4.
- [19] Unger N, Zheng Y, Yue X, et al. Mitigation of ozone damage to the world's land ecosystems by source sector. *Nat Clim Chang* 2020;10:134–7.
- [20] Zhang DQ, Hui DF, Luo YQ, et al. Rates of litter decomposition in terrestrial ecosystems: Global patterns and controlling factors. *J Plant Ecol* 2008;1:85–93.
- [21] Han TF, Huang WJ, Liu JX, et al. Different soil respiration responses to litter manipulation in three subtropical successional forests. *Sci Rep* 2015;5:18166.
- [22] Chen X, Chen HYH. Global effects of plant litter alterations on soil CO₂ to the atmosphere. *Glob Chang Biol* 2018;24:3462–71.
- [23] Yue X, Unger N. The Yale Interactive terrestrial Biosphere model: Description, evaluation and implementation into NASA GISS ModelE2. *Geosci Model Dev* 2015;8:2399–417.
- [24] Yue X, Unger N. Fire air pollution reduces global terrestrial productivity. *Nat Commun* 2018;9:5413.
- [25] Yu Z, Ciais P, Piao S, et al. Forest expansion dominates China's land carbon sink since 1980. *Nat Commun* 2022;13:5374.
- [26] Lawrence DM, Hurtt GC, Arneeth A, et al. The land use model intercomparison project (LUMIP) contribution to CMIP6: Rationale and experimental design. *Geosci Model Dev* 2016;9:2973–98.
- [27] Farquhar GD, Caemmerer SV, Berry JA. A biochemical-model of photosynthetic CO₂ assimilation in leaves of C₃ species. *Planta* 1980;149:78–90.
- [28] Ball JT, Woodrow IE, Berry JA. A model predicting stomatal conductance and its contribution to the control of photosynthesis under different environmental conditions. In: Biggins J, editor. *Progress in Photosynthesis Research*. Dordrecht: Nijhoff; 1987. p. 221–4.
- [29] Clark DB, Mercado LM, Sitch S, et al. Joint UK Land Environment Simulator (JULES), model description—Part 2: Carbon fluxes and vegetation dynamics. *Geosci Model Dev* 2011;4:701–22.
- [30] Xu YS, Shang B, Feng ZZ, et al. Effect of elevated ozone, nitrogen availability and mesophyll conductance on the temperature responses of leaf photosynthetic parameters in poplar. *Tree Physiol* 2020;40:484–97.
- [31] Friedlingstein P, Jones MW, O'Sullivan M, et al. Global carbon budget 2021. *Earth Syst Sci Data* 2022;14:1917–2005.
- [32] Weedon GP, Balsamo G, Bellouin N, et al. The WFDEI meteorological forcing data set: WATCH Forcing Data methodology applied to ERA-Interim reanalysis data. *Water Resour Res* 2014;50:7505–14.
- [33] Friedl MA, Sulla-Menashe D, Tan B, et al. MODIS Collection 5 global land cover: Algorithm refinements and characterization of new datasets. *Remote Sens Environ* 2010;114:168–82.
- [34] Jiang F, Chen JM, Zhou LX, et al. A comprehensive estimate of recent carbon sinks in China using both top-down and bottom-up approaches. *Sci Rep* 2016;6:22130.
- [35] Amiro BD, Barr AG, Barr JG, et al. Ecosystem carbon dioxide fluxes after disturbance in forests of North America. *J Geophys Res Biogeosci* 2010;115:G00k02.
- [36] Brodrribb TJ, Powers J, Cochard H, et al. Hanging by a thread? Forests and drought. *Science* 2020;368:261–6.
- [37] Yuan WP, Zheng Y, Piao SL, et al. Increased atmospheric vapor pressure deficit reduces global vegetation growth. *Sci Adv* 2019;5:eaax1396.
- [38] Qiu ZX, Feng ZK, Song YN, et al. Carbon sequestration potential of forest vegetation in China from 2003 to 2050: Predicting forest vegetation growth based on climate and the environment. *J Clean Prod* 2020;252.
- [39] Huang Y, Sun WJ, Qin ZC, et al. The role of China's terrestrial carbon sequestration 2010–2060 in offsetting energy-related CO₂ emissions. *Natl Sci Rev* 2022;9.
- [40] Xu H, Yue C, Zhang Y, et al. Forestation at the right time with the right species can generate persistent carbon benefits in China. *Proc Natl Acad Sci USA* 2023;120:e2304988120.
- [41] Cai WX, He NP, Li MX, et al. Carbon sequestration of Chinese forests from 2010 to 2060 spatiotemporal dynamics and its regulatory strategies. *Sci Bull* 2022;67:836–43.
- [42] Ge J, Pitman AJ, Guo WD, et al. Impact of revegetation of the Loess Plateau of China on the regional growing season water balance. *Hydrol Earth Syst Sci* 2020;24:515–33.
- [43] Lu N, Tian HQ, Fu BJ, et al. Biophysical and economic constraints on China's natural climate solutions. *Nat Clim Chang* 2022;12:847–53.
- [44] Shi XR, Zheng YX, Lei Y, et al. Air quality benefits of achieving carbon neutrality in China. *Sci Total Environ* 2021;795:148784.
- [45] Tong D, Cheng J, Liu Y, et al. Dynamic projection of anthropogenic emissions in China: Methodology and 2015–2050 emission pathways under a range of socio-economic, climate policy, and pollution control scenarios. *Atmos Chem Phys* 2020;20:5729–57.
- [46] Lu M, Yue X, Lei Y, et al. Deep cut of anthropogenic nitrogen oxides emissions to mitigate ozone vegetation damages in China. *Atmos Environ* 2023;293:119454.
- [47] Zhang FF, Xing J, Zhou Y, et al. Estimation of abatement potentials and costs of air pollution emissions in China. *J Environ Manag* 2020;260:110069.
- [48] Osiecka A, Minogue PJ, Miwa M, et al. Nutrient removals by pine straw harvesting in slash pine plantations in Florida. *For Sci* 2020;66:314–25.
- [49] Matsushima M, Chang SX. Vector analysis of understory competition, N fertilization, and litter layer removal effects on white spruce growth and nutrition in a 13-year-old plantation. *For Ecol Manag* 2006;236:332–41.
- [50] Alam A, Kellomaki S, Kilpelainen A, et al. Effects of stump extraction on the carbon sequestration in Norway spruce forest ecosystems under varying thinning regimes with implications for fossil fuel substitution. *Glob Change Biol Bioenergy* 2013;5:445–58.
- [51] Sathre R, Gustavsson L. Time-dependent climate benefits of using forest residues to substitute fossil fuels. *Biomass Bioenergy* 2011;35:2506–16.
- [52] Zeng N, Hausmann H. Wood vault: Remove atmospheric CO₂ with trees, store wood for carbon sequestration for now and as biomass, bioenergy and carbon reserve for the future. *Carbon Bal Manag* 2022;17:2.
- [53] Li MX, He NP, Xu L, et al. Eco-CCUS: A cost-effective pathway towards carbon neutrality in China. *Renew Sust Energ Rev* 2023;183:113512.
- [54] Wei YM, Kang JN, Liu LC, et al. A proposed global layout of carbon capture and storage in line with a 2 °C climate target. *Nat Clim Chang* 2021;11.
- [55] Meinshausen M, Lewis J, Nicholls Z, et al. 1.9°C: New COP26 pledges bring projected warming to below 2°C for the first time in history. Nov. 10th, 2021 <https://data.climateaction.com.au/ndc/20211103-ClimateResource-below2C.pdf>.
- [56] Lee J-Y, Marotzke J, Bala G, et al. Future global climate: Scenario-based projections and near-term information. In: Masson-Delmotte V, Zhai P, Pirani A, et al., editors. *Climate Change 2021: The Physical Science Basis Contribution of Working Group I to the Sixth Assessment Report of the Intergovernmental Panel on Climate Change*. Cambridge: Cambridge University Press; 2021.



Xu Yue is a professor at the School of Environmental Science and Engineering, Nanjing University of Information Science and Technology. He develops vegetation models that incorporate the ecological impacts of air pollution, investigates the interactions among the atmospheric environment, land ecosystems, and climate systems, and explores the potential of nature-based solutions to enhance land carbon sinks.



Hong Liao is a professor at the School of Environmental Science and Engineering, Nanjing University of Information Science and Technology. She has been developing aerosol and gas-phase chemistry modules, aiming to unravel the spatiotemporal variations of air pollutants and to simulate climate change caused by such changes. She also explores chemical mechanisms for ozone formation and the strategies for synergistic control of surface-layer PM_{2.5}.